Numerical Methods in Civil Engineering, 5-3 (2021) 13-22

Numerical Methods in Civil Engineering

Journal Homepage: https://nmce.kntu.ac.ir/

A multi-objective optimization approach to optimal sensor placement of irregular LSF structures

Mohammad Reza Hamedi[*], Masoud Mohammadgholiha[**], Hamid Reza Vosoughifar[***], Nadia Hamedi[****]

ARTICLE INFO

APPLICABLE PAPER

Article history:
Received:
November 2020.
Revised:
January 2021.
Accepted:
February 2021..

Keywords:
Optimal Sensor Placement (OSP), Lightweight Steel Framing (LSF), Structural Health Monitoring (SHM), MAC Criteria

Abstract:

In recent years, lightweight steel framed (LSF) structures are designed to resist fire, earthquakes, and storm events. This system has entered the field of construction due to advantages of light members. Based on these advantages, such a system is also used for buildings with special importance. Structural health monitoring (SHM) implements a damage detection and characterization strategy for engineering structures. In the present study, a multi-objective numerical method for optimal sensor placement based on the combination of Modal Assurance Criteria (MAC) and maximum stress has been proposed. Genetic Algorithm (GA) was employed to determine the location of sensors on the structure based on the structural dynamic response of the LSF system. To show the efficiency of the proposed method, a very large irregular museum building, which was built by using LSF system, has been considered. To improve the proposed method, dominant frequencies are identified and the number of sensors is decreased using the Fourier Transform (FT) of the ground motions time history. Results show that the proposed method can provide the optimal sensor locations and remarkably reduce the number of required sensors and also improve their optimum location.

1. Introduction

Lightweight Steel Framing (LSF) systems have been used for low and medium rise residential, industrial, and commercial building construction. Cold-formed steel (CFS) is used because of its advantages, including lightness, being dimensionally stable, non-flammable, termite and borer proof, durable, lightweight, and 100% recyclable. Several experimental and analytical studies on Cold-Formed Steel (CFS) profiles, members and framing systems have been conducted recently. Xu and Tangorra [1] carried out an experimental study on vibration characteristics of cold-formed steel supported lightweight residential floor systems. Al-Kharat and Rogers [2] presented an experimental overview of the inelastic performance of CFS sections.

In their study, sixteen cold-formed steel strap braced walls that were not designed according to a strict capacity-based design, were subjected to monotonic and reversed cyclic loading. Results showed that under the condition of ignoring capacity design principles, the overall system ductility severely decreased. Dan Dubina [3] summarizes the research activities carried out in the last few years at the Politechnica University of Timisoara in order to evaluate the performance of light steel framed structures. In this paper, monotonic and cyclic tests on full-scale shear panels, tests on connection details, and in situ ambient vibration tests on a house under construction are reviewed and concluded. Moghimi and Ronagh [4] presented the techniques to improve the behavior of cold-formed steel structures. They studied the performance of different light-gauge cold-formed steel strap-braced stud wall arrangements. In their study, twenty full-scale 2.4 m × 2.4 m specimens were subjected to cyclic loading.

** Ph.D. Student, Department of Civil Engineering, Science and Research Branch, Islamic Azad University, Tehran, Iran.*
*** Corresponding Author: Ph.D. student, Department of Electrical, Electronic, and Information Engineering, University of Bologna, Bologna, Italy, Email: m.mohammadgholiha@unibo.it*
**** Associate professor, Department of Civil Engineering, Science and Research Branch, Islamic Azad University, Tehran, Iran.*
***** Graduate Student, Department of Architecture, Qazvin Branch, Islamic Azad University, Qazvin, Iran.*

Damage in a structural system is defined as an undesirable change in its behavioral characteristics [5]. Indeed, damage can be considered as the changes in a system that will unfavorably affect future operations. There are different methods of detecting damage in a structure. One of the oldest methods is based on the structural modal parameters [6, 7]. Modal parameters are frequency and structural mode shapes, which produce relatively acceptable results. Su et al. [8] located damaged stories in a shear building via reduction of natural frequencies of the sub-structure that included the damaged story. There are more accurate methods of damage detection, which are based on curvature mode shape and modal strain energy [9, 10, and 11]. For instance, Cao et al. [12] detected multiple cracks in a cantilever beam using curvature mode shape. The difference between wavelet transform coefficients before and after damage [13, 14, and 15] is used as a criteria of damage. The main part of health monitoring and control of structures is parameter identification. Mode shapes and modal frequencies are kinds of structural parameters that can be used to describe the dynamic behavior of a structural system. The reliability of modal parameter identification strongly depends on the robustness of the measured vibration data, which depends on the locations of sensors in the structure [16]. As a result, determining the optimal sensor placement (OSP) has a significant role in an accurate modal parameter identification process. Numerous methods have been advanced for solving the optimal sensor placement problem. Carne and Dohrmann [17] developed a famous algorithm called modal assurance criteria (MAC), which was initialized with a small set of sensors, and added sensors to reduce the off-diagonal MAC elements. Effective independent (EFI) method was presented to select a group of locations which contributed significantly to the linear independence of the target modal partitions. Hemez and Farhat [18] presented an algorithm in which the effective independence method is combined with the strain energy of the structure. Roohi and Hernandez [19] developed an optimal sensor placement methodology by minimizing the uncertainty of dynamic response reconstruction. An optimization problem was formulated to select the optimal measurement matrix subject to maximum inter-story drift estimation variance bounded by a maximum allowable variance [20, 21]. The optimization object function was defined based on the power spectral density of displacement estimation error obtained using an extended model-based observer [22]. Miller [23] computed a Gaussian quadrature formula using the gain functional as a weight function. In this study, the author assumed that the nodes of the Gaussian quadrature formula indicated the optimal location of sensors. The approach utilized in this paper was to attempt to obtain the best possible numerical approximation to the integrals appearing in the control law for a fixed number of measurements of the state (sensor outputs). Kammer [24] proposed an effective independence (EFI) method based on the contribution of each sensor location to the linear independence of the identified modes. Hiramoto et al. [25] used the explicit solution of the algebraic Riccati equation to determine the optimal sensor/actuator placement for active vibration control. Wouwer et al. [26] measured the independence of the sensor responses and presented the formula as the optimality criteria. Worden and Burrows [27] used several methods to determine an optimal sensor distribution based on the curvature data. In addition, Cobb and Liebst [28] and Shi et al. [29] have reported the optimal sensor placement (OSP) to detect structural damages. Shokouhi and Vosoughifar [30] proposed a novel numerical approach, which is called transformed time history, to frequency domain (TTFD) algorithm, in order to improve optimal sensor placement (OSP) procedure. In the present study, a new method for optimal sensor placement of LSF structures is proposed. The proposed index is defined as the combination of modal assurance criteria (MAC) values and maximum stresses of structural elements. Thus, the optimal sensor locations are determined based on both the linear and nonlinear behavior of LSF structures. To do so, a very large irregular museum building, built using LSF system, has been modeled using the finite element method (FEM) and followed by performing the modal and nonlinear time history (NTH) analysis by considering the effects of near-fault earthquakes. For the first time, the effect of ground motion directions on the seismic response of the LSF structures is considered. Finally, the genetic algorithm (GA) is selected to act as the solution to the optimization formulation in the selection of the best sensor placement.

2. Description of the proposed method

An optimal sensor arrangement can minimize the number of sensors required, increase accuracy, and provide the best possible performance of the structural health monitoring system [31]. For these reasons, a numerical approach based on the combination of modal assurance criteria (MAC) values and maximum stresses is proposed here to determine the optimal number of sensors.

Carne and Dohmann [17] thought that the MAC is an ideal scalar constant by which the correlation between two modal vectors can be obtained. The MAC is defined as Eq(1), where ϕ_i and ϕ_j are the mode shape vectors for the i-th and j-th modes, respectively, and the superscript T represents the transpose of the vector. MAC_{ij} represents the cosine of the angle between those two vectors, and the smaller the cosine, the more distinguishable the shape vectors.

$$MAC_{ij}=\frac{(\phi_i^T\phi_j)^2}{(\phi_i^T\phi_i)(\phi_j^T\phi_j)} \quad (1)$$

In the above formulation, the element values of the MAC matrix range between 0 and 1 is presented, where 0 indicates that there is little or no correlation between the off-diagonal element MAC_{ij} ($i \neq j$) (the modal vector easily distinguishable) and 1 indicates that there is a high degree of similarity between the modal vectors (the modal vector fairly indistinguishable).

For a traditional optimal sensor configuration, the MAC matrix would be diagonal. Thus, the size of the off-diagonal elements of MAC is a criteria for the performance of OSP, and can be considered as an indication of the objective function. However, in the present study, such criteria have not been used. The method used here is to initialize the selection of the sensor set, based on the maximum values of the off-diagonal MAC elements, leading to the selection of modes with high similarity. In other words, the use of MAC in LSF structures was performed with the aim of creating the sensors layout at locations with higher values of displacements in the combination of modes. It is worth mentioning that in low-rise LSF structures, the effect of higher modes on the structural response is not significant for one to easily assign the initial sensor location based on the first three modes [31]. With this in mind, the preliminary sensor locations are determined. Then, a nonlinear time history (NTH) analysis is performed to determine the maximum stress in structural elements. Now, the objective function is formed as a combination of the MAC and the maximum stress criteria. Finally, the genetic algorithm (GA) is adopted to determine the final locations of the sensors.

2.1. Initial sensor assignment by using MAC values

To begin with, after assigning the specific numbers to the structural nodes, the modal analysis is performed to determine the structural modal parameters. Then, as shown in Fig.1, the displacement of the points at the different modes and corresponding coordinate values are obtained.

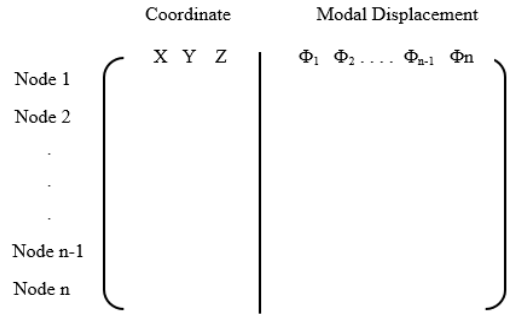

Fig. 1: Displacement of the points at the different modes and corresponding coordinate values

It is noteworthy to mention that, in Fig.1, the Euclidean norm of the nodal displacement values at each mode is considered as the modal displacement. Then, the MAC values for each pair of modes are calculated, and the results are stored in a matrix (see Fig.2).

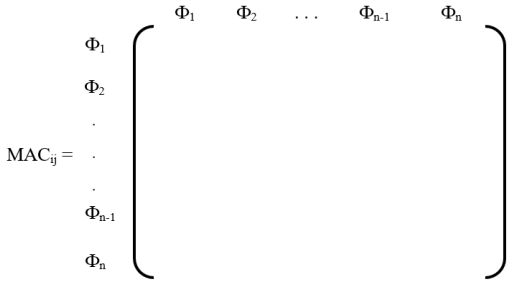

Fig. 2: MAC values

The MAC fitness function is given as Eq (2):

$$f=1-\max\left(\text{abs}\left(MAC_{ij}\right)\right), \quad i\neq j \tag{2}$$

The above objective function is used to determine the highest MAC values for identifying the critical modes with similar motions. In fact, locations with highest displacement in the combination of modes are utilized for sensor placement. As a result, such points have the maximum displacement during an earthquake.

After forming the MAC matrix, modes with a particular MAC value are considered, and modal displacement is calculated using the root mean square of values. Hence, the displacement of a node in the first mode with the same displacement of the node in the second mode is combined. Such work is performed for all nodes, and its values are stored in a matrix. Then, the nodes with the maximum combined displacement are selected as the initial location of sensors. Moreover, the corresponding MAC values are considered as a term in the forming of the objective function. It should be noted that the duplicated values are detected and deleted.

2.2. Determining of maximum stress in LSF structure

In this section, the nonlinear time history (NTH) analysis is performed to obtain the maximum stress values in the structure. Then, the stress values and corresponding coordinate values are stored in a matrix for further analysis. The final fitness function is given as Eq (3):

$$\min z=W_1\sum_{i=1}^{n} d_i D_i^{min}-W_2\sum_{j=1}^{n} f_j c_j \tag{3}$$

In the above equation, d_i is the normalized stress, D_i is the distance of the initial location of sensors from the structural nodes, f_j is the sensors coefficient, whose value is one or zero (where 0 indicates that the sensor is off and 1 indicates that the sensor is on), and c_j is the MAC value. W_1 and W_2 are the weight functions of stress and MAC criteria, respectively. It should be noted that since the amount of stress term (in the fitness function) is always higher than that

of the MAC, these two terms are unified by using the weight coefficient.

2.3. Optimization of sensor locations by genetic algorithm (GA)

In order to find the optimal solution of the objective function given in the previous section, the genetic algorithm (GA) is used. The GA is widely used for optimization based on evolutionary ideas of genetics and natural selection. The GA is a computational intelligence method to the OSP problem that reaches the global optimum effectively. The GA approach starts with a discrete set (also called generation) of design vectors (also called individuals, chromosomes or strings). Through three main operations (selection, crossover, and mutation), it modifies the current set towards generating a better generation of design points. Every individual is uniquely identified by a code called chromosome, which is mapped to a certain value of the objective function, representing the fitness of the individual. In every generation, the fittest chromosomes are given a greater chance of survival and pass their genes to the next generation [31]. A general genetic algorithm is shown in Fig.3.

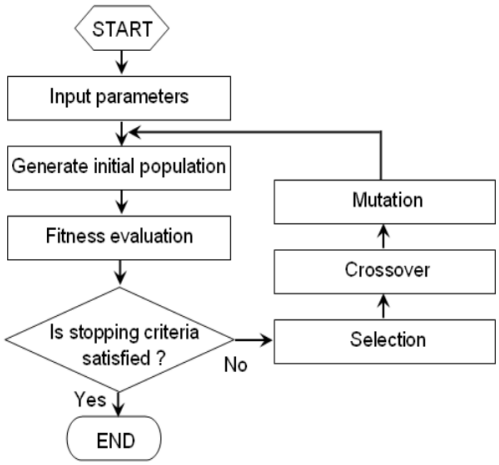

Fig. 3: Principle of the genetic algorithm

As previously mentioned, in this research, the genetic algorithm has been used to locate the optimal placement of sensors. In our case, the individuals of the initial population are binary codified hypothetical sensor sets: the optimal sensor combination candidates. The number of genes in this chromosome is equal to the number of selected sensors based on the MAC criteria for the optimization procedure. Fig.4 shows the chromosome which is used in the GA algorithm.

Sensor number	1	2	3	4	5	…	K
Chromosome	1	0	0	1	1	…	1

Fig. 4: Chromosomes used in the present study

There is a number on top of each gene, which represents the gene number of the sensor. The number of genes used in this chromosome is equal to K (the number of sensors selected based on the MAC criteria). In each gene, the number is set to 0 or 1, where 0 indicates that the sensor is off and 1 indicates that the sensor is on. Fig.5 shows an example of the chromosome used in this algorithm.

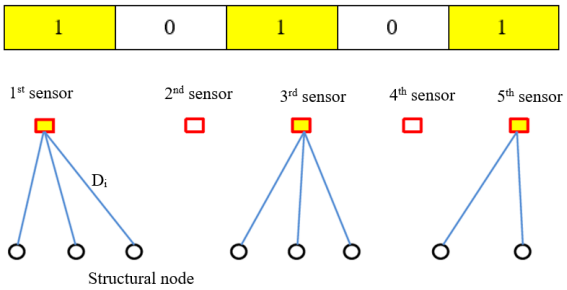

Fig. 5: Operation of a chromosome

The proposed algorithm is as follows:

1. The setup of the number of input variables include the coordinates of the structural element nodes, the stresses obtained from nonlinear time history (NTH) analysis, and the nodes of the structure which have the most displacement in the combination of modes. The sensor location candidates are decision variables (i.e., all possible DOFs of the structure).
2. Creating the initial population in which each generation consists of 30 chromosomes. Such a population is usually randomly generated and can be any desired size, from only a few individuals to thousands.
3. Calculation of the cost function for the chromosomes of the initial population.
4. Optimization by using the Genetic Algorithm.

3. Description of the LSF structure

In the present study, a 4-story irregular LSF structure was modeled, and three dimensional (3D) analysis was performed. The preliminary finite element (FE) model was established using structural analysis software SAP2000. Beam and shell elements were utilized for frame modeling. However, in order to investigate the nonlinear behavior of structural elements, the final FE modeling was performed in ABAQUS. Steel sections were defined using the wire elements. Therefore, truss elements were used for stud modeling, while beam elements were used for braces. Modal and explicit dynamic analyses were also carried out to study the dynamic behavior of the LSF structure.

A 3D view of the FE model is depicted in Fig.6. The aforementioned building has various plans, and the LRFD design algorithm was used for the design procedure based on the AISI standard [32]. The considered building is used as a museum located at the high damage risk zone of Tehran

city. Therefore, health monitoring of this structure is plausible, and it can be an appropriate example of wide-range LSF structural behavior. The main frame of the wall panels was made of LSF elements, and top and bottom tracks were U204/2.0 (that is, U shape with 204 × 100 dimensions and 2.0-mm thickness), while studs were C200/2.0 profiles, fixed at each end to tracks with self-drilling self-tapping screws. In this building, board sheets of cement as cladding were placed in a horizontal position with a useful width of 1,200 mm. The board sheets were fixed to the wall frame using special self-tapping screws. The number of screws is determined in a way to avoid failure at strap end fixings and facilitate yielding. 10-mm oriented strand board (OSB) panels (1,200 × 2,440 mm^2) were placed only on the 'external' side of the building similarly as the gypsum panels were put in internal spaces of the building, and fixed to the frame using bugle head self-drilling screws of d = 4.2-mm diameter at 1-mm intervals.

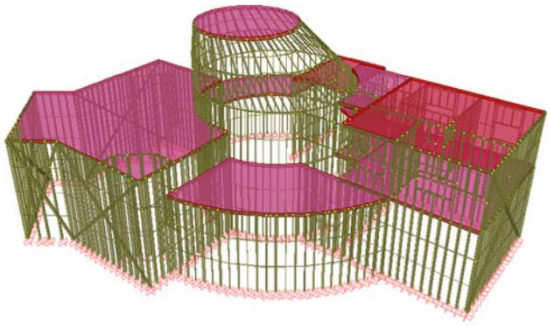

Fig. 6: The finite element model of the LSF structure [26]

Table.1 presents the material properties of the LSF structure.

Table 1: Material properties

Parameter	Value
Yield strength (MPa)	344.21
Ultimate tensile strength (MPa)	447.18
Modulus of elasticity (GPa)	190
Poisson's ratio	0.30

The vibration properties were calculated by performing modal analysis. Table.2 presents the first five frequencies of the LSF structure.

Table 2: Modal frequencies calculated using FE model

Mode n.	Period (s)	Frequency (Hz)
1	0.63	1.58
2	0.52	1.92
3	0.49	2.04
4	0.24	4.16
5	0.19	5.26

Fig.7 illustrates the first three fundamental mode shapes of LSF structure.

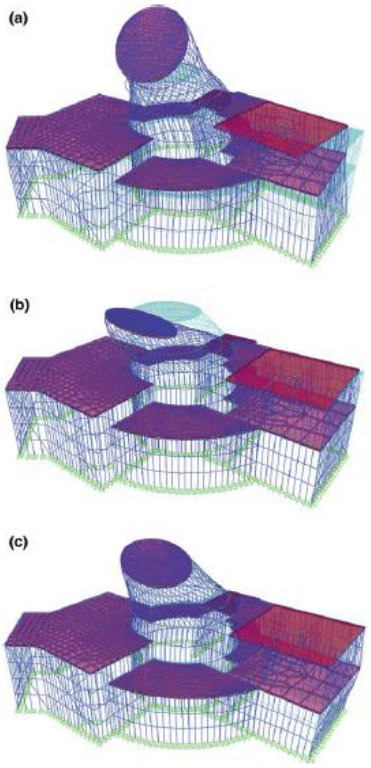

Fig. 7: The first three fundamental mode shapes of the LSF structure (a first mode, b second mode, c third mode) [26]

3.1 Nonlinear time history (NTH) analysis of LSF structure

One of the most important challenges in analyzing irregular structures is considering the effects of earthquakes on structural responses. In this study, in order to select the appropriate earthquake records based on three criteria of magnitude, distance, and type of soil, the TOPSIS method is used [33]. Table.3 and Table.4 show the selected earthquake records, including near-field and far-field earthquakes, for the NTH analysis.

Table 3: Near-field ground motion records

Earthquake	Station
LANDERS	1158 ,JOSHUA
Duzce, Turkey	1058 Lamont 1058
NORTHR-MUL	90013Beverly Hills - 14145 Mulhol

Table 4: Far-field ground motion records

Earthquake	Station
CHICHI	CHY086
LANDERS	23 Cool water
NORTHRIDGE	24278 castaic-old ridge route

Since seismic forces may be applied in any horizontal direction to the structure, the regulations have applied criteria for considering these effects. However, in this research, a study was conducted to find the critical direction of the irregular LSF structure. In the first step, earthquake records were applied in the main directions of the structure. Afterward, the analysis was repeated by rotating the pairs of accelerograms record in the counter-clockwise direction with a small angle of 5 degrees until reaching the angle of 90 degrees. In applying the accelerogram record in the main directions, the structure has shown acceptable stability during an earthquake, and only the local buckling of a few studs occurred, which does not structural instability. However, when the varying degrees of rotation was applied to the accelerogram record, local buckling and displacement of the structural elements increased, resulting in collapse (see Fig.8). To reduce the excessive displacement caused by an earthquake, the dimensions of the cross section of the braces was increased by about 10%, and the structure was re-analyzed, leading to the elimination of the structural instability. Table.5 shows the procedure of applying the rotation for the Northridge accelerogram record.

Table 5: Base shear values based on the angle changes for Northridge record

Rotation Angle (Degrees)	Base Shear (Tonf) in x-direction	Base Shear (Tonf) in y-direction	Changes Applied for the next analysis
0	36.27	24.57	-
5	37.78	24.65	-
10	collapse	-	Increase the cross section of the braces
10	41.13	21.92	-
15	42.71	27.7	-
. . .			
25	collapse	-	Increase the cross section of the braces
25	41.38	27.37	-
. . .			
90	50.21	45.26	-

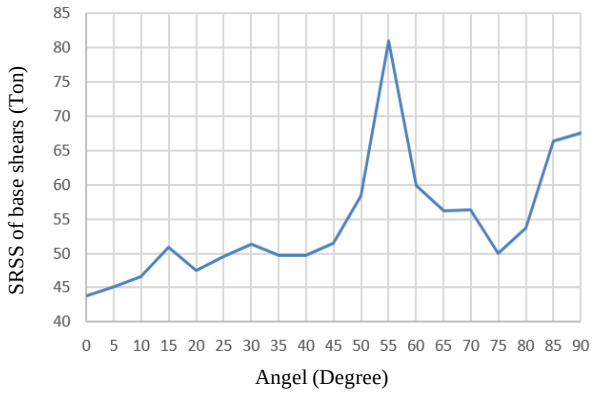

Fig. 8: SRSS of perpendicular base shears vs. rotation angle for Northridge record

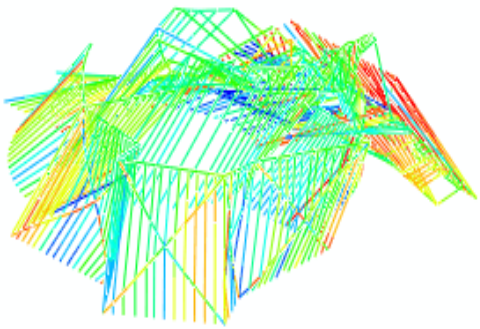

Fig. 9: The collapse of the structure in torsional displacements under Northridge record

As shown in Fig.8, the critical angle under which the maximum base shear has occurred is obtained to apply the ground motion records. Fig.9 shows the collapse of the LSF structure under an angle of 10 degrees.

4. Implementation of the proposed method for the LSF structure

As mentioned in the previous sections, the first step is to perform the modal analysis in order to obtain the mode shapes of the LSF structure. Then, the initial placement of sensors is located by using the MAC values. Nonlinear time history (NTH) analysis is performed to obtain the structural element stresses. After that, the fitness function is formed as the combination of the MAC and stresses values. Finally, the genetic algorithm (GA) is selected to act as the solution to the optimization formulation in the selection of the best sensor placement. Fig. 10 depicts the convergence graph of GA algorithm for the near-field Northridge ground motion.

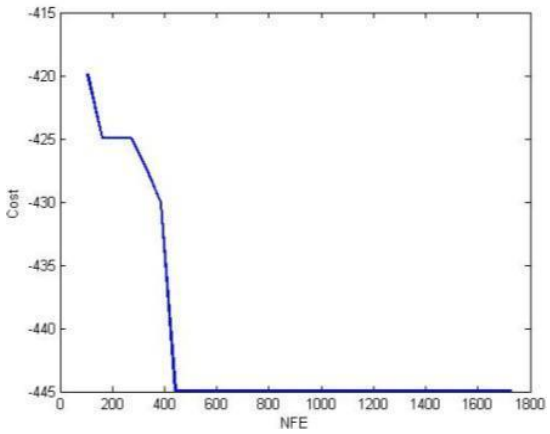

Fig. 10: Convergence graph of GA algorithm for the near-field Northridge ground motion

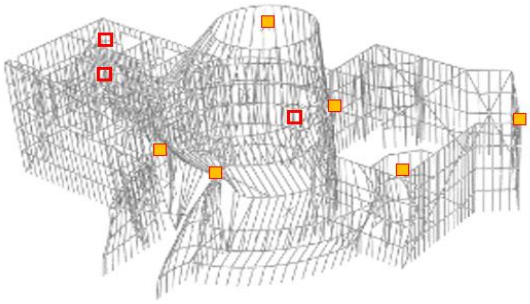

Fig. 11: 3D view of the location of sensors under Northridge far-field record

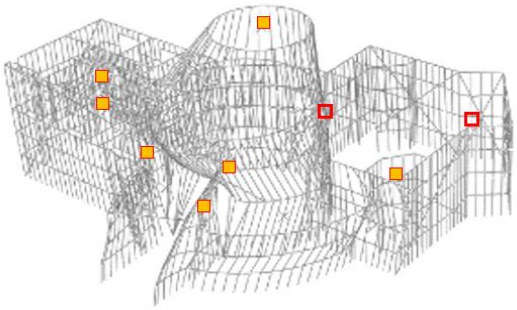

Fig. 12: 3D view of the location of sensors under Northridge near-field record

Fig.11 and Fig.12 show the optimal location of sensors for the LSF structure under the Northridge far-field and near-field records, respectively. It should be noted that in these figures, the solid squares indicate that the sensor is on (it is necessary), and the hollow squares indicate that the sensor is off (it is not necessary).

5. Reducing the number of sensors using the Fourier transform (FT) of the ground motion records

It is obvious that each earthquake induces a structure at certain frequencies and shows a certain degree of Fourier amplitude. Frequency values with higher Fourier amplitudes are more important in structural behavior. To estimate the range of critical frequencies, we can compare the frequency content of the various earthquakes and, firstly, evaluate the accuracy of the modal analysis of the previous steps, and secondly, choose the more critical frequencies from the various frequencies obtained from the modal analysis.

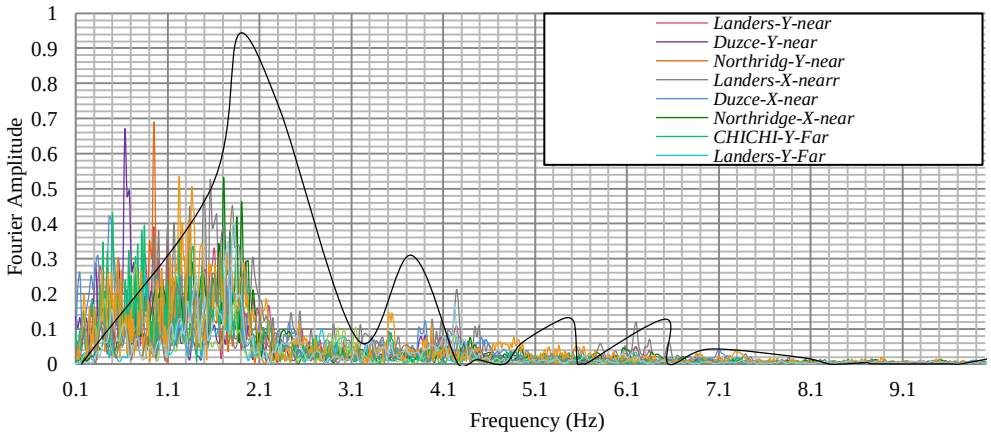

Fig. 13: Comparison of the Fourier Amplitude with the modal mass, in terms of frequency

As a result, modes with higher reliability are selected, which are more compatible with the possible earthquakes' characteristics in/on the site. Fig.13 shows the normalized modal mass for the frequencies obtained from the modal analysis and Fourier spectrum of the ground motion records. As shown in Fig.13, the structure in the NTH analysis is excited at lower frequencies than the modal frequencies obtained from the modal analysis. By comparing the NTH graph with the modal analysis, several higher-frequency modes were eliminated. Furthermore, other modes removed in the modal analysis were retained.
In the following, the frequencies obtained from the Fourier amplitude spectrum of the ground motion records are used instead of the selected frequencies based on the modal analysis to form the MAC matrix and perform the optimal sensor placement procedure.

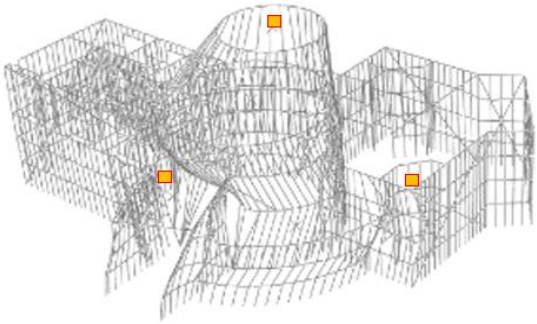

Fig. 14: 3D view of the location of sensors using FT method for all the ground motions

Using such a method, fewer frequencies are selected than the modal analysis. Furthermore, increasing the reliability of these modes leads to finding fewer points for locating the sensors in the structure and is more cost-effective. Fig.14 shows the optimal location of sensors for the LSF structure under the near-field and far-field ground motion records. As shown in Fig.14, the number of required sensors is dramatically reduced, thanks to the FT technique. Furthermore, the effect of ground motions is not significant in sensor placement, as the same results were obtained for all the ground motions.

6. Conclusion

Large and complex civil structures are being placed in extreme conditions such as wind, earthquake, traffic load, to name but a handful. As a result, the need for robust and accurate health monitoring techniques continues to grow. Considering this, careful selection and placement of sensors are the critical issues in the construction and implementation of an effective structural health monitoring system. This paper presents a new method to determine the optimal placement of sensors for health monitoring of irregular LSF structures, based on the combination of modal assurance criteria (MAC) values and maximum stresses. The conclusions are summarized as follows:

- In order to determine the seismic response and the critical direction of irregular LSF structures, a very large LSF building with irregularity in plan and height, is selected and the nonlinear time-history (NTH) analysis is performed by considering the effects of near-fault earthquakes. The results of the analysis show that, in the case in which the structure is subjected to the earthquake records in the main directions, the maximum base shear values of the structure is approximately 60% higher than the maximum base shear for the earthquake record in other directions, indicating the high sensitivity of the seismic response of such structures to the earthquake direction.

- In the monitoring of irregular LSF structures, it should be noted that in the presence of lateral load resisting elements, including braces with very strong sections and beyond seismic requirements, if these members remain in their linear behavior, damage to the structure is due to damage to the connection, which is also due to the increase of the dynamic base shear. In this case, monitoring and controlling maximum stresses near the connections can be used for monitoring purposes. By reducing the cross-section of the brace and allowing the use of the nonlinear capacity of the brace, the base shear of the structure has been reduced significantly. Still, the local and global instabilities of the structure due to the large displacement of the diaphragms have mainly destroyed the structures. In this case, monitoring and controlling of displacements and accelerations can be the objective of structural health monitoring systems.

- In this study, dynamic data (acceleration, velocity, and displacement) and mechanical data (stress and strain) are considered simultaneously. Accordingly, the initial layout strategy of intelligent sensors, for example, fiber optic sensors, has been created using a two-objective cost function including the maximum values of the MAC criteria and the maximum stresses of the structure during an earthquake. The genetic algorithm (GA) is selected to act as the solution to the optimization formulation in the selection of the best sensor placement. The results of optimization algorithms indicate the need for more sensors to record data for near-field earthquakes in comparison to far-field earthquakes. This is due to the more destructive effects of near-field earthquakes on LSF structures, which have high natural frequencies.

- Using dominant frequencies obtained from the Fourier transform (FT) of the ground motion records has a significant role in reducing the number of monitoring

sensors. In fact, the modes which are not excited during an earthquake are identified and removed. In this study, using this technique, the number of sensors required to record data was reduced by about 60%, significantly reducing the time and cost of health monitoring of such structures. Moreover, the effect of ground motions is not significant in sensor placement using the FT method, as the same results were obtained for all the ground motions.

References

[1] Xu L, Tangorra FM. (2007). Experimental investigation of lightweight residential floors supported by cold-formed steel C-shape joists. Journal of constructional steel research, 63(3), 422-35.

[2] Al-Kharat M, Rogers CA. (2007). Inelastic performance of cold-formed steel strap braced walls. Journal of Constructional Steel Research, 63(4), 460-74.

[3] Dubina D. (2008). Behavior and performance of cold-formed steel-framed houses under seismic action. Journal of Constructional Steel Research, 64(7-8), 896-913.

[4] Moghimi H, Ronagh HR. (2009). Performance of light-gauge cold-formed steel strap-braced stud walls subjected to cyclic loading. Engineering Structures, 31(1), 69-83.

[5] Glisic B, Inaudi D. (2008). Fibre optic methods for structural health monitoring. John Wiley & Sons.

[6] Doebling SW, Farrar CR, Prime MB, Shevitz DW. (1996). Damage identification and health monitoring of structural and mechanical systems from changes in their vibration characteristics: a literature review. Los Alamos National Lab, NM (United States).

[7] Turner JD, Pretlove AJ. (1988). A study of the spectrum of traffic-induced bridge vibration. Journal of Sound and Vibration, 122(1), 31-42.

[8] Su WC, Huang CS, Hung SL, Chen LJ, Lin WJ. (2012). Locating damaged stories in a shear building based on its sub-structural natural frequencies. Engineering Structures, 39, 126-38.

[9] Karami Mohammadi, R., Khalaj, M., Mohammadgholiha, M. (2018). Curvature Method to Detect Location and Depth of a Plastic Zone in Frame Members during an Earthquake. Journal of Numerical Methods in Civil Engineering, 3(2), 1-12.

[10] Ciambella J, Vestroni F, Vidoli S. (2011). Damage observability, localization and assessment based on Eigen frequencies and eigenvectors curvatures. Smart Structures and Systems, 8(2), 191-204.

[11] Kim JT, Ho DD, Nguyen KD, Hong DS, Shin SW, Yun CB, Shinozuka M. (2013). System identification of a cable-stayed bridge using vibration responses measured by a wireless sensor network. Smart Structures and Systems, 11(5), 533-53.

[12] Cao M, Radzieński M, Xu W, Ostachowicz W. (2014). Identification of multiple damage in beams based on robust curvature mode shapes. Mechanical Systems and Signal Processing, 46(2), 468-80.

[13] Amaravadi VK, Rao VS, Koval LR, Derriso MM. (2001, August). Structural health monitoring using wavelet transforms. In Smart Structures and Materials 2001: Smart Structures and Integrated Systems (Vol. 4327, pp. 258-270). International Society for Optics and Photonics.

[14] Castro E, Garcia-Hernandez MT, Gallego A. (2006). Damage detection in rods by means of the wavelet analysis of vibrations: Influence of the mode order. Journal of sound and vibration, 296(4-5), 1028-38.

[15] Castro E, Garcia-Hernandez MT, Gallego A. (2007). Defect identification in rods subject to forced vibrations using the spatial wavelet transform. Applied Acoustics, 68(6), 699-715.

[16] Papadimitriou C. (2004). Optimal sensor placement methodology for parametric identification of structural systems. Journal of sound and vibration, 278(4-5), 923-47.

[17] Carne TG, Dohrmann CR. (1995, February). A modal test design strategy for model correlation. In Proceedings-Spie. The International Society For Optical Engineering (pp. 927-927). SPIE INTERNATIONAL SOCIETY FOR OPTICAL.

[18] Hemez FM, Farhat C. (1994, January). An energy based optimum sensor placement criteria and its application to structural damage detection. In Proceedings-SPIE The International Society for Optical Engineering (pp. 1568-1568). SPIE INTERNATIONAL SOCIETY FOR OPTICAL.

[19] Roohi, Milad, Eric M. Hernandez. (2020). Performance-based post-earthquake decision making for instrumented buildings. Journal of Civil Structural Health Monitoring. 10, 775–792.

[20] Roohi, Milad, Eric M. Hernandez, and David Rosowsky. (2020). Reconstructing element-by-element dissipated hysteretic energy in instrumented buildings: application to the Van Nuys Hotel testbed. arXiv: Signal Processing: arXiv:2002.12426.

[21] Roohi, Milad, Eric M. Hernandez, and David Rosowsky. (2019) .Nonlinear Seismic Response Reconstruction in Minimally Instrumented Buildings—Validation Using NEESWood Capstone Full-Scale Tests. Structural Health Monitoring. 10.12783/shm2019/32390

[22] Roohi, Milad, et al. (2020). An extended model-based observer for state estimation in nonlinear hysteretic structural systems. Mechanical Systems and Signal Processing 146: 107015.

[23] Miller RE. (1998). Optimal sensor placement via Gaussian quadrature. Applied mathematics and computation, 97(1), 71-97.

[24] Kammer DC. (1991). Sensor placement for on-orbit modal identification and correlation of large space structures, Journal of Guidance, Control and Dynamics, 14 (2), 251-259.

[25] Hiramoto K, Doki H, Obinata G. (2000). Optimal sensor/actuator placement for active vibration control using explicit solution of algebraic Riccati equation. Journal of Sound and Vibration, 229(5), 1057-75.

[26] Wouwer AV, Point N, Porteman S, Remy M. (2000). An approach to the selection of optimal sensor locations in distributed parameter systems. Journal of process control, 10(4), 291-300.

[27] Worden K, Burrows AP. (2001). Optimal sensor placement for fault detection. Engineering structures, 23(8), 885-901.

[28] Cobb RG, Liebst BS. (1997). Sensor placement and structural damage identification from minimal sensor information. AIAA journal, 35(2), 369-74.

[29] Shi ZY, Law SS, Zhang LM. (2000). Optimum sensor placement for structural damage detection. Journal of Engineering Mechanics, 126(11), 1173-9.

[30] Shokouhi SK, Vosoughifar HR. (2013). Optimal sensor placement in the lightweight steel framing structures using the novel TTFD approach subjected to near-fault earthquakes. Journal of Civil Structural Health Monitoring, 3(4), 257-67.

[31] Holland JH. (1975). Adaptation in natural and artificial systems. An introductory analysis with application to biology, control, and artificial intelligence. Ann Arbor, MI: University of Michigan Press, 439-44.

[32] Cold-Formed Steel Design Manual and Specification Bundle, 2010. AISI, USA.

[33] Hwang CL. et Yoon, K. .(1981). Multiple Attribute Decision Making, Methods and Applications: a State of the Art Survey. Lecture notes in economics and mathematical systems, Springer-Verlag, New York, NY.